Numerical analysis of the bonding behavior between a basalt fiber reinforced polymers rebar and concrete

Luis Felipe Oliveira Santos
Pontifícia Universidade Católica de Campinas
PUC-Campinas
Campinas, Brasil
luis.ofsantos@gmail.com

Nádia Cazarim da Silva Forti
Pontifícia Universidade Católica de Campinas
Pró-Reitoria de Pesquisa e Pós-Graduação
Campinas, Brasil
nadia.cazarim@puc-campinas.edu.br

***Abstract* —** *This study aims to simulate the bonding behavior between a Basalt Fiber Reinforced Polymers rebar (BFRP) and concrete using numerical methods. Fiber reinforced polymers rebars (FRP) are materials composed of fiber (glass, basalt, etc.) and a polymeric matrix. They are light, non-corrosive and tensile-resistant materials. A quarter of the model was modeled due to symmetry. The parameters used for the concrete simulated the elastic and plastic behavior of the material, using the "Elastic" and "Concrete Damage Plasticity" models, respectively. The rebar was parameterized considering linear elastic behavior until its rupture. The adhesion between the materials used cohesion parameters (stiffness coefficients K) and the damage caused by the pullout. Different parameters used in the simulation influence the stress-slip behavior of the BFRP rebar and the concrete. The influences of these parameters are studied and analyzed. The present study verifies the great influence of the shear stiffness coefficients in the simulations (maximum adhesion stress and slip). The influence of this parameter on the stress distribution in concrete was also observed. The model created a good stress-slip behavior, but it is still necessary to improve the parameters used in this study. To run a simulation, the student version of the Abaqus was used, marketed by SIMULIA, a trademark owned by Dassault Systèmes S.A.*

Keywords — abaqus; pull-out; BFRP; FRP; FEM; simulação

I. INTRODUCTION

The use of rebars as reinforcement for concrete structures is possible due to the solidarization between the materials, allowing the rebar not to slip. Adhesion between concrete and rebar happens through chemical bonding, friction, mechanical locking and the pressure between faces caused by temperature change and concrete shrinkage [2].

Steel rebars used as reinforcement for concrete structures are susceptible to corrosion processes in presence of chloride ions. Fiber reinforced polymer rebars (FRP) appear as an alternative. Its high resistance to corrosion, high strength / weight ratio in relation to steel, are great advantages for civil construction [3] [16].

The disadvantages of fiber reinforced polymer rebars are: low elastic modulus, low ductility and lower shear strength [16].

Adhesion is an important element in the study of structural behavior, so it is necessary to know the failure of adhesion between materials. Usually the failure is related to the rupture of the concrete due to shear and the rupture of the ribs in the rebar. However, it can also occur due to cracking in the concrete, which is more fragile [1].

The stress-slip behavior of concrete and rebar can be defined by a linear ascending branch (of KT inclination), an increasing and non-linear branch, followed by a stress drop in the post-rupture behavior, Fig. 1 [5].

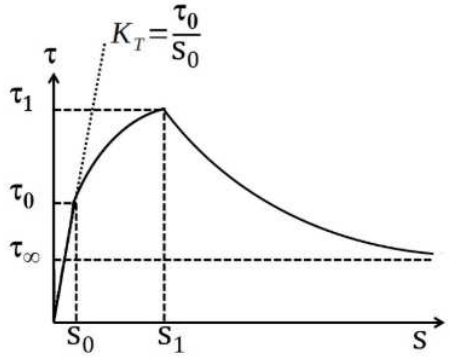

Fig. 1. Stress-slip behavior [5]

Numerical simulation can be a complement to experimental research. It assists in analysis that are not possible to be done experimentally. In addition, simple models simulation allows you to model, simulate and analyze more complex models, such as beam and column frames.

A numerical model that simulates the stress-slip behavior during pullout is composed of two main components, concrete and rebar.

Concrete has a good compression performance. The stress-strain behavior of the material is linear up to approximately 40% of its compressive strength. This behavior can be obtained experimentally or estimated from mathematical expressions, such as Hognestad [8] [9].

Basalt fiber reinforced polymers rebars (BFRP) do not have a defined yield point like steel. Andrea et al. [10] experienced a

BFRP rebar subjected to tensile load and observed a largely linear behavior.

Using surface-to-surface contact conditions allows to simulate the stress-slip behavior. The contact simulation makes use of stiffness (K) parameters in three directions: one in the normal direction and two in the shear directions; and damage onset and damage evolution parameters [18].

II. NUMERICAL MODEL

The pull-out model was simulated using data obtained from the bibliography, taken from Shen et al. [11].

The test performed by Shen et al. [11] uses a BFRP rebar with a diameter of Ø14 mm, tensile strength of 1000 MPa, strain of 2.08%, elastic modulus 48000 MPa and length of 400 mm. The concrete used has a compressive strength of 43.6 MPa.

The concrete specimen has a cubic shape with dimensions of 150 mm. The length bonded between the rebar and the concrete was 5Ø (70 mm) located in the middle third of the model, Fig. 2.

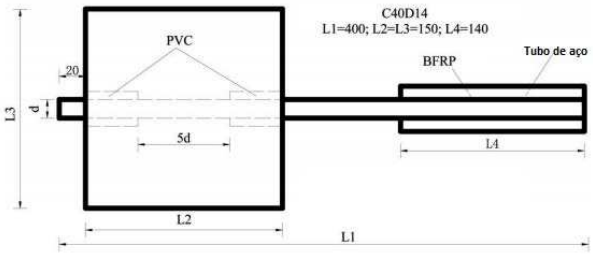

Fig. 2. Pullout test model [11].

A. Concrete

The article did not provide the stress-strain behavior of the concrete used in the experimental test. So, in this work, the Hognestad method was adopted to estimate it. Equation (1) was used for strains between the linear phase limit stress strain (40% of the compressive strength) and the ultimate stress strain. Equation (2) referring to post peak stress strains, as proposed by Zhu et al. [12].

$$\sigma = f_c' \times \left(\left(2 \times \frac{\varepsilon}{\varepsilon_0} \right) - \left(\left(\frac{\varepsilon}{\varepsilon_0} \right)^2 \right) \right) \quad (1)$$

$$\sigma = f_c' \times \left(1 - 0{,}15 \times \left(\frac{\varepsilon - \varepsilon_0}{\varepsilon_{cu} - \varepsilon_0} \right) \right) \quad (2)$$

With the Hognestad mathematical model it was possible to estimate the stress-strain behavior of concrete, Fig. 3.

Fig. 3. Estimated stress-strain behavior for concrete.

The linear behavior of the graph was parameterized in Abaqus using the elastic modulus. The concrete elastic modulus was not provided by the author, so it was estimated as directed by ABNT NBR 6118 [20]. For the plastic behavior, the "Concrete Damage Plasticity" (CDP) method was used.

The parameters used by Labibzadeh et al. [19] were used to characterize the plasticity of concrete: dilatation angle (ψ), eccentricity (e), ratio between the compressive strength under biaxial load and the uniaxial compressive strength (fb0 / fc0), ratio of the second invariant stress in the traction meridian for compressive (K) and viscosity (μ), TABELA I.

TABELA I. PARAMETERS OF THE CDP METHOD [19]

CDP – Plastic behavior				
ψ	***e***	***fb0/fc0***	***K***	***M***
35	0.1	1.12	0.67	0

To simulate the compressive behavior, inelastic strain and damage were calculated, TABELA II.

TABELA II. PARAMETERS FOR CHARACTERIZING THE COMPRESSIVE BEHAVIOR OF CONCRETE

Compressive behavior		
Stress	***Inelastic strain***	***Damage***
17,44	0,00E+00	0,00
19,00	8,64E-05	0,00
20,00	9,74E-05	0,00
21,00	1,09E-04	0,00
22,00	1,22E-04	0,00
23,00	1,36E-04	0,00
24,00	1,51E-04	0,00
25,00	1,68E-04	0,00
26,00	1,85E-04	0,00
27,00	2,05E-04	0,00
28,00	2,25E-04	0,00
29,00	2,48E-04	0,00
30,00	2,72E-04	0,00
31,00	2,98E-04	0,00
32,00	3,27E-04	0,00
33,00	3,58E-04	0,00
34,00	3,93E-04	0,00
35,00	4,31E-04	0,00
36,00	4,73E-04	0,00
37,00	5,21E-04	0,00
38,00	5,74E-04	0,00
39,00	6,36E-04	0,00

Compressive behavior		
Stress	***Inelastic strain***	***Damage***
40,00	7,09E-04	0,00
41,00	7,97E-04	0,00
42,00	9,12E-04	0,00
43,60	1,39E-03	0,00
42,00	2,13E-03	0,04
41,00	2,59E-03	0,06
40,00	3,05E-03	0,08
39,00	3,50E-03	0,11
38,00	3,96E-03	0,13
37,00	4,42E-03	0,15
36,00	4,88E-03	0,17
35,00	5,34E-03	0,20
34,00	5,80E-03	0,22
33,00	6,26E-03	0,24
32,00	6,71E-03	0,27
31,00	7,17E-03	0,29
30,00	7,63E-03	0,31
29,00	8,09E-03	0,33
28,00	8,55E-03	0,36
27,00	9,01E-03	0,38
26,00	9,47E-03	0,40
25,00	9,93E-03	0,43
24,00	1,04E-02	0,45
23,00	1,08E-02	0,47
22,00	1,13E-02	0,50
21,00	1,18E-02	0,52
20,00	1,22E-02	0,54
19,00	1,27E-02	0,56
18,00	1,31E-02	0,59
17,00	1,36E-02	0,61
16,00	1,41E-02	0,63
15,00	1,45E-02	0,66

Equations (3) and (4) were used to calculate the inelastic strain and damage [9].

$$\varepsilon_c^{in,h} = \varepsilon_c - \frac{\sigma_c}{E_0} \tag{3}$$

$$d_c = 1 - \frac{\sigma_c}{\sigma_{cu}} \tag{4}$$

The average tensile strength, according to ABNT NBR 6118 [20], and the fracture energy were used to simulate the tensile behavior. According to Abaqus Inc. [17] the fracture energy of concrete can be from 0.04 N/mm to 0.12 N/mm depending on its compressive strength. Therefore, a fracture energy of 0.12 N/mm was adopted.

B. BFRP rebar

According to Brisotto et al. [1], the rupture of the rebar-concrete interface is usually associated with the failure of the concrete. So, assuming that the rebar will not break, a linear-elastic behavior was adopted in its stress-strain graph.

The linear-elastic behavior of rebar was simulated using the elastic modulus provided by the author and the Poisson coefficient.

For glass fiber reinforced polymers (GFRP) the Poisson ratio can range from 0.20 to 0.22. For an epoxy matrix it can range from 0.20 to 0.33 [21]. It was not possible to define or calculate the Poisson coefficient mathematically, but the value of 0.20 was adopted for the simulation.

C. Adhesion

With a plot digitizer software, the graphical data provided by Shen et al. [11] was extracted , Fig. 4.

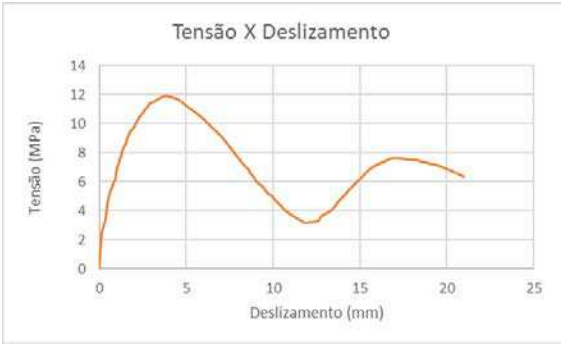

Fig. 4. Digitized tension-slip behavior.

The cohesion and damage were used to simulate the behavior of contact between materials.

Abaqus uses the stiffness coefficients K (Knn, Kss and Ktt) to simulate the cohesive behavior of materials. The Knn coefficient is the normal stiffness to the work plane and Kss and Ktt are the shear stiffness of the work plane.

The Ktt coefficient can be calculated from the inclination of the linear branch of the tension-slip graph obtained experimentally. So defined as the ratio between the stress in the linear branch and the slip [5].

For the shear stiffness coefficients (Kss and Ktt) two values were used. As directed by Rolland et al. [5], the first was estimated at 20.5 MPa/mm. Seeking to converge the simulation results with the expected results, the second was calculated as the ratio between the maximum adhesion stress by the respective slip, estimated at 3.20 MPa/mm, TABELA III.

TABELA III. DATA FOR ADHERENCE CHARACTERIZATION

Kss = Ktt (1)	Kss = Ktt (2)	Energia de Fratura
20.50 kN/mm	3.20 kN/mm	66.70 kN.mm

Another parameter considered in Abaqus is damage, separated in initial and evolution damage. The initial damage is separated by three stress components, one normal and two shears. For the shear component, the maximum bond strength experimentally obtained was adopted. The damage evolution was parameterized by the contact fracture energy (Gf). The fracture energy is calculated per unit area in the stress-slip post-stress peak graph, Fig. 5, as available in ABAQUS Inc. documentation [18].

Fig. 5. Contact fracture energy per unit area .

D. *Boundary conditions*

A quarter of the model was adopted due to the symmetry. To restrict the movement of the faces, support conditions were added in the x direction of the yz plane and in the y direction of the xz plane, Fig. 6.

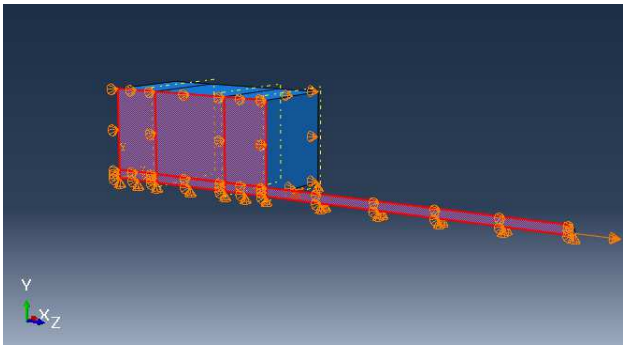

Fig. 6. Boundary condition applied in the yz plane.

A boundary condition was applied in the z direction of the xy plane, Fig. 7.

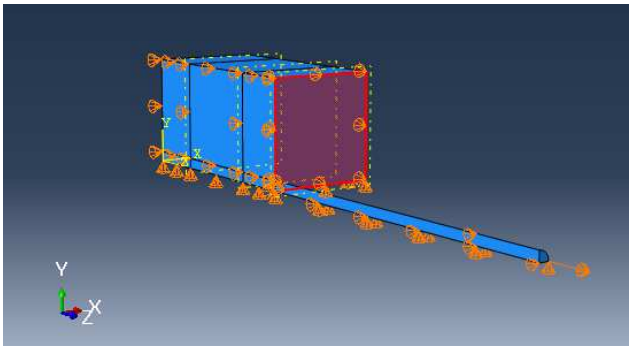

Fig. 7. Boundary condition applied to the concrete face in the xy plane.

To simulate the pullout, a displacement was applied at the end of the rebar, Fig. 8.

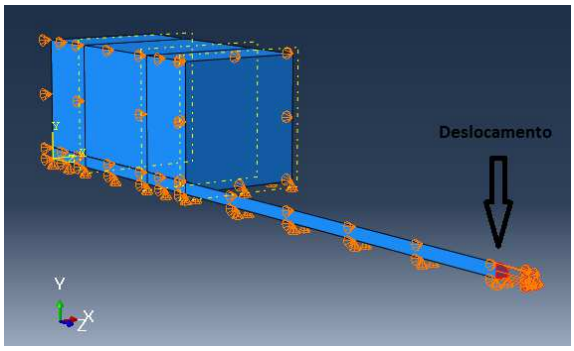

Fig. 8. Displacement applied at the end of the rebar.

III. RESULTS AND DISCUSSION

The expected model presented a non-linear stress-slip behavior, with a maximum adhesion stress of 11.88 MPa and a slip of 3.73 mm.

Adopting the first hypothesis for the shear stiffness coefficient (Kss = Ktt = 20.50 MPa/mm), the bond stress was 11.91 MPa and the slip was 0.59 mm, Fig. 9.

The difference between the stress obtained and the expected stress was less than 1%, but the displacement showed a great difference.

When we used the second hypothesis for the shear stiffness coefficient (Kss = Ktt = 3.20 MPa/mm), the model showed better agreement of results. An adhesion tension of 11.90 MPa and a slip of 3.71 mm, Fig. 9.

Graphically, the models presented a different inclination in the pre-peak stress branch, due to the different shear stiffness coefficients adopted.

The numerical models presented a graphic evolution in the stress-slip behavior different from that observed experimentally, Fig. 9. The numerical model proved to be similar to the typical pull-separation behavior, available in the Abaqus Inc. documentation [18]. Defined by an initial linear elastic behavior, followed by damage initiated when contact stresses (or slips) satisfy the adopted criterion [18].

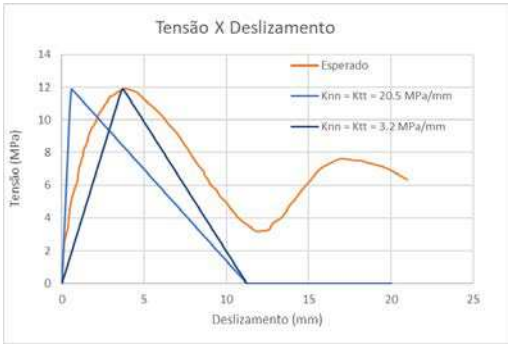

Fig. 9. Comparison of stress-slip behavior.

According to Brisotto et al. [1], the stress-slip behavior based only on the bonding stresses does not consider the confinement effects, changing the bonding behavior. An elasto-plastic interface model is needed to consider the confinement.

Although we observe a big difference in the stress-slip behavior when we change the bond strength, the same does not happen with the stress distribution in concrete.

When we use a shear stiffness coefficient of 20.50 MPa/mm, the maximum acting stress in concrete of 1.347 MPa is observed, Fig. 10.

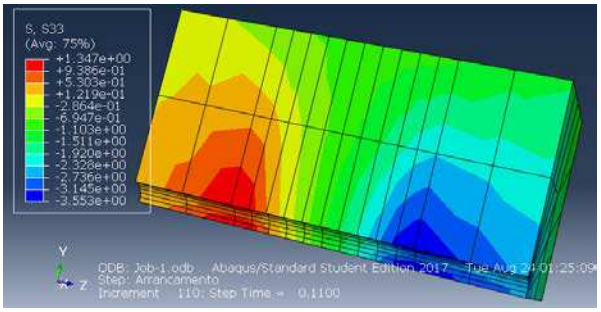

Fig. 10. Stress distribution across concrete when Kss = Ktt = 20.50 MPa/mm.

When we adopt a shear stiffness coefficient of 3.20 MPa/mm, the maximum acting stress in concrete of 1.346 MPa is observed, Fig. 11.

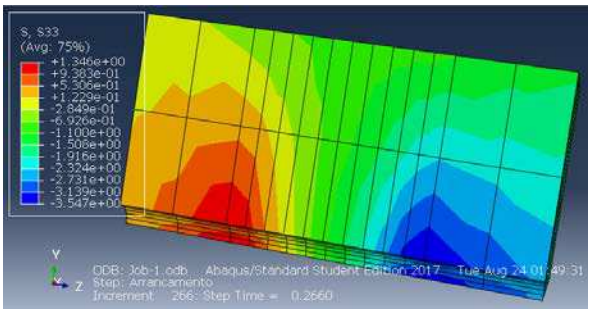

Fig. 11. Stress distribution across concrete when Kss = Ktt = 3.20 MPa/mm.

The stress distribution in the concrete was very similar in both analyses, even with the great difference in the stress-slip behavior. This suggests little influence of this parameter on the stress distribution along the model.

IV. Conclusions

When the shear stiffness coefficient was 3.20 MPa/mm, the model showed good agreement with the stress-slip data.

The shear stiffness coefficient defines the graphic inclination of the ascending branch in the slip bond stress behavior.

The stress-slip behavior simulated using Abaqus showed a different graphic development than expected, but similar to a typical tension-separation model.

The shear stiffness coefficient did not cause great influence on the stress distribution along the concrete, when we observed the moment related to adhesion failure.

ACKNOWLEDGMENT

The authors thank CNPq for the scholarship.

REFERENCES

[1] BRISOTTO, D. S.; BITTENCOURT, E.; BESSA, V. M. R. D. Simulation of interface behavior between FRP bars and concrete by an elastic-plastic theory via FEM. Revista IBRACON de Estruturas e Materiais, v. 11, n. 6, p. 1381–1390, 2018.

[2] AKISHIN, PAVEL; KOVALOVS, ANDREJS; KULAKOV, VLADIMIR; ARNAUTOV, ALEXANDER. Finite element modelling of slipage between FRP rebar and concrete in pull-out test. p. 6, 2014.

[3] KOBAYASHI, K.; IIZUKA, T.; KURACHI, H.; ROKUGO, K. Corrosion protection performance of High Performance Fiber Reinforced Cement Composites as a repair material. Cement and Concrete Composites, v. 32, n. 6, p. 411–420, 2010.

[4] REFAI, AHMED EL; AMMAR, MOHAMED-AMINE; MASMOUDI, RADHOUANE – “Bond Performance of Basalt Fiber-Reinforced Polymer Bars to Concrete”, 2014.

[5] ROLLAND, ARNAUD; ARGOUL, PIERRE; BENZARTI, KARIM; QUIERTANT, MARC; CHATAIGNER, SYLVAIN; KHADOUR, AGHIAD. Analytical and numerical modeling of the bond behavior between FRP reinforcing bars and concrete. Construction and Building Materials, v. 231, n. January, 2020.

[6] ČERVENKA, VLADIMÍR; JENDELE, LIBOR; ČERVENKA, JAN. ATENA Program Documentation Part 1. p. 1–33, 2020.

[7] BI, Q.; WANG, H. Bond strength of BFRP bars to basalt fiber reinforced high-strength concrete. Advances in FRP Composites in Civil Engineering - Proceedings of the 5th International Conference on FRP Composites in Civil Engineering, CICE 2010. Anais...2011

[8] GUJEL, D. A.; KAZMIERCZAK, C. S.; MASUERO, J. R. Stress-strain curve of concretes with recycled concrete aggregates: analysis of the NBR 8522 methodology. Revista IBRACON de Estruturas e Materiais, v. 10, n. 3, p. 547–567, 2017.

[9] HAFEZOLGHORANI, MILAD; HEJAZI, FARZAD; VAGHEI, RAMIN; JAAFAR, MOHD SALEH BIN; KARIMZADE, KEYHAN. Simplified damage plasticity model for concrete. Structural Engineering International, v. 27, n. 1, p. 68–78, 2017.

[10] SERBESCU, ANDREEA; GUADAGNINI, MAURIZIO; PILAKOUTAS, KYPROS. Mechanical Characterization of Basalt FRP Rebars and Long-Term Strength Predictive Model. Journal of Composites for Construction, v. 19, n. 2, p. 04014037, 2015.

[11] SHEN, DEJIAN; OJHA, BINOD; SHI, XIANG; ZHANG, HUI; SHEN, JIAXIN. Bond stress-slip relationship between basalt fiber-reinforced polymer bars and concrete using a pull-out test. Journal of Reinforced Plastics and Composites, v. 35, n. 9, p. 747–763, 2016.

[12] ZHU, CHAOQI; WANG, QI; JIA, YONGGANG; JIANG, BEI; LI, WEITENG; SHAO, XING; et al. Numerical analysis on the ultimate bearing capacity and parameter selection of U-shaped confined concrete short column. Electronic Journal of Geotechnical Engineering, v. 20, n. 26, p. 13051–13062, 2015.

[13] COSTA, MÁRIO HENRIQUES ARAGÃO; JÚNIOR, MARCELO SILVA MEDEIROS; JÚNIOR, EVANDRO PARENTE. Análise de Estruturas de Concreto Armado Considerando Dano e Plasticidade. XIII SIMMEC 2018 - Vitória - ES, 2018.

[14] BELIAEV, M., SEMENOV, A., SEMENOV, S., BENIN, A. Simulation of Pulling the Reinforcing Bar from Concrete Block with Account of Friction and Concrete Damage. Petersburg, 2016.

[15] DORIA, M. R.; SALES, A. T. C; ANDRADE, N. F. de A. Bond strength between stell-concrete and between concretes with different ages in structural rehabilitation. Revista IBRACON de Estruturas e Materiais, v. 8, n. 5, p. 604–624, 2015.

[16] DIAZ, I.; LARRÚA, R.; WAINSHTOK, H.; MACKCHASER, M.. Simplified methods to determine shear strength in reinforced concrete beams with fiber-reinforced polymers exposed to fire. Revista Ingenieria de Construccion, v. 36, n. 1, p. 97–106, 2021.

[17] ABAQUS Inc. Concrete damaged plasticity. Disponível em: <https://abaqus-docs.mit.edu/2017/English/SIMACAEMATRefMap/simamat-c-concretedamaged.htm>. Acessado em 14/08/2021.

[18] ABAQUS Inc. Contact cohesive behavior. Disponível em: <https://abaqus-

docs.mit.edu/2017/English/SIMACAEITNRefMap/simaitn-c-cohesivebehavior.htm#simaitn-c-cohesivebehavior-t-DamageEvolutionDefinition-sma-topic23__simaitn-c-cni-cohesive-linear-softening>. Acessado em 15/08/2021.

[19] LABIBZADEH, MOJTABA; ZAKERI, MOJTABA; SHOAIB, ABDOL ADEL. A new method for CDP input parameter identification of the ABAQUS software guaranteeing uniqueness and precision. International Journal of Structural Integrity, v. 8, n. 2, p. 264–284, 2017.

[20] ASSOCIAÇÃO BRASILEIRA DE NORMAS TÉCNICAS. NBR 6118 – Projeto de estruturas de concreto – Procedimento. Rio de Janeiro, 2014

[21] CASTRO, Protasio F. Barras de FRP: avaliando o módulo de elasticidade não destrutivamente. Polímeros, v. 7, n. 2, p. 58–65, 1997.